

Current research on local scour at bridge pier in Viet Nam

By Tran Dinh Nghien

University of Transport and Communication Viet Nam

Abstract: An investigation of the maximum scour depth at cylindrical bridge pier has been conducted by studying the horseshoe vortex system developed at the base of the pier before scouring & at equilibrium scour condition for clear-water scour & live-bed scour & three practical design relation have been suggested. Delta-wing-like passive device to reduce local scour depth and flexible mat as the best protection device against scour have been carried out. Runoff & total stream flow in Viet Nam is also briefly presented.

Before dealing with the current research on local scour at bridge piers in Viet Nam, runoff & total stream flow in Viet Nam is briefly presented here.

When a storm occurs, a portion of rainfall infiltrates into the ground & some portion may evaporates. The rest of flow as a thin sheet of water over the land surface which is termed as overland flow & the interflow together with the ground flow form all the total stream flow.

The average annual total stream flow during the period of time 1961 - 1998 in Viet Nam (in the north, up to Quang Binh province; in the south, from Quang Binh province to all southern provinces) is estimated roughly about 847 km^3 , it is approximately 2% equivalent to global rivers annual total stream flow & nearly equal to annual flow rate, $Q_0=26850 \text{ m}^3/\text{s}$.

The river system in Viet Nam, depending on its course & the topographical feature of its run, can be divided into 10 systems with catchment area and total stream flow given in the table 1 as follows:

Table 1. Total stream flow in Viet Nam

Order	River system	Area, km ²			Total stream flow, km ³								
		Inland Viet Nam	Inflow from out border	Total	Average			Probability 75%			Probability 90%		
					Inland	Inflow	Total	Inland	Inflow	Total	Inland	Inflow	Total
1	Ky Cung Bang	11280	1980	13260	7.3	1.7	9.0	5.63	1.53	7.16	4.7	1.2	5.9
2	Thai Binh	15180	-	15180	9.7	-	9.7	7.90	-	7.90	6.3	-	6.3
3	Hong	72700	82300	155000	81.3	45.2	126.0	72.70	39.6	112.00	68.0	36.0	104.0
4	Ma – Chu	17600	10800	28400	14.0	5.6	19.6	12.00	4.5	16.00	9.3	3.8	13.1
5	Ca	17730	9470	27200	17.8	4.4	22.2	13.00	3.7	16.70	9.5	3.3	12.8
6	Thu Bon	10350	-	10350	20.1	-	20.1	17.40	-	17.40	13.0	-	13.0
7	Ba	13900	-	13900	9.5	-	9.5	7.74	-	7.74	6.4	-	6.4
8	Dong Nai	37400	6700	44100	32.8	3.5	36.3	28.70	2.9	31.60	23.8	2.4	26.2
9	Mekong	68824	726176	795000	53.0	447.0	500.0	42.00	404.0	446.00	37.5	377.5	415.0
10	All others rivers	96723	-	96723	94.5	-	94.5	75.90	-	75.90	68.0	-	68.0
Total river system		361687	837426	1199113	340	507.4	846.9	282.97	456.23	738.4	246.5	424.2	670.7

The values in the Table 1 were obtained by using available data of the 177 gauging stations with catchment area ranged from less than 100 km² to larger than 500 km².

Of the total stream flow at 847 km³, 59% is Mekong river system, 14.9% is red river system (using data at Son Tay gauging station in the period of time 1902 to 1988), 4.29% is Dong Nai river system, nearly 2% is sum of Ca, Ma & Thu Bon rivers system, about 1% is sum of Ky Cung – Bang, Thai Binh & Ba rivers system, the remaining 26.8% being in the all other small & medium rivers system.

River systems in Viet Nam receive only run off due to rainfall and were affected by many factor forming flow such as climatological conditions, storm characteristics, basin characteristics, storage characteristics; among all the factors monsoons play the most important role because most amount of water recorded have occurred during the monsoon season.

Current research on local scour at bridge pier in Viet Nam

1. Introduction

It is well known that when a blunt nosed bridge pier is placed in an erodible river bed, the flow pattern in the river around the pier is significantly changed, the flow upstream of the pier will undergo a three-dimensional separation & this separated layer will roll up to form a vortex system upstream of the pier. The ends of this vortex system are swept downstream toward infinity, increasing the rotational velocities in the vortex core and when viewed from above this vortex system has a characteristic shape, namely a the horseshoe vortex system. The shear stress distribution around the pier drastically changed due to the formation of a horseshoe vortex leads to the scouring of sediment around the pier as well as forming a scour hole, which, in turn, changes the flow pattern and shear. Bridge & road engineers have concerned with this problem since a long time, numerous studies have been conducted and equations developed with a view to adequately predict the maximum scour depth at bridge pier. However, most of these equations were developed using laboratory data & sometimes tested using limited field data, relatively little attention have been focused on the mechanism of the scouring process. Several investigators to the understanding of the mechanism of scour in the steady flow such as Baker (1979, 1980); Belick (1973); Breusers et al (1977); Lauser & Toch (1956); Melville & Raudkivi (1977); Neill (1964); Posey (1949, 1950); Qadar (1981); Roper et al (1967); Altunin, Kurganovich & Petrov (1977); Bogomolov, Altunin et al (1975); Juravlev (1978, 79, 80, 83); Nakagawa & Suzuki (1975).

The main aim of the present report to show investigation having been carried out to fill in some gaps in the understanding of bridge pier scour as well as scour protection with the flowing aspects:

- Flow chart for description of the local scour research.
- A description of model study in general.
- A comparison of the theoretical work with field data & suggestion for design relations to be developed.
- The protection against scour in addition, briefly.

Circular pipes with diameters of 5cm, 6cm & round-nosed wooden log of 5cm wide, 18cm long & 45cm high were used as piers model for the studies on the determination of the size of the horseshoe vortex, whereas, only round-nosed wooden log mentioned above was used for scour study and for delta-wing-like passive device applied to the leading nose of pier model mounted on mobile bed of 14cm thick uniform bed having medium size of 0.155mm and geometric standard deviation $\sigma_g = 1.22$ as the representative particle size for all experiments.

Firstly, some idea of the size of the horseshoe vortex at the bottom of pier model mounted on a flat plate under different flow conditions have been investigated through flow visualization by paint impression in the first phase because of that precise measurement of the size of the vortex is too difficult due to the horseshoe vortex being quasi-periodical & multiple vortex system. In the second phase, the flat plate has been replaced by an erodible sand bed.

2. Description of the local scour research

The flow chart for performing the research on local scour at bridge pier in steady flow is presented here in Fig.1.

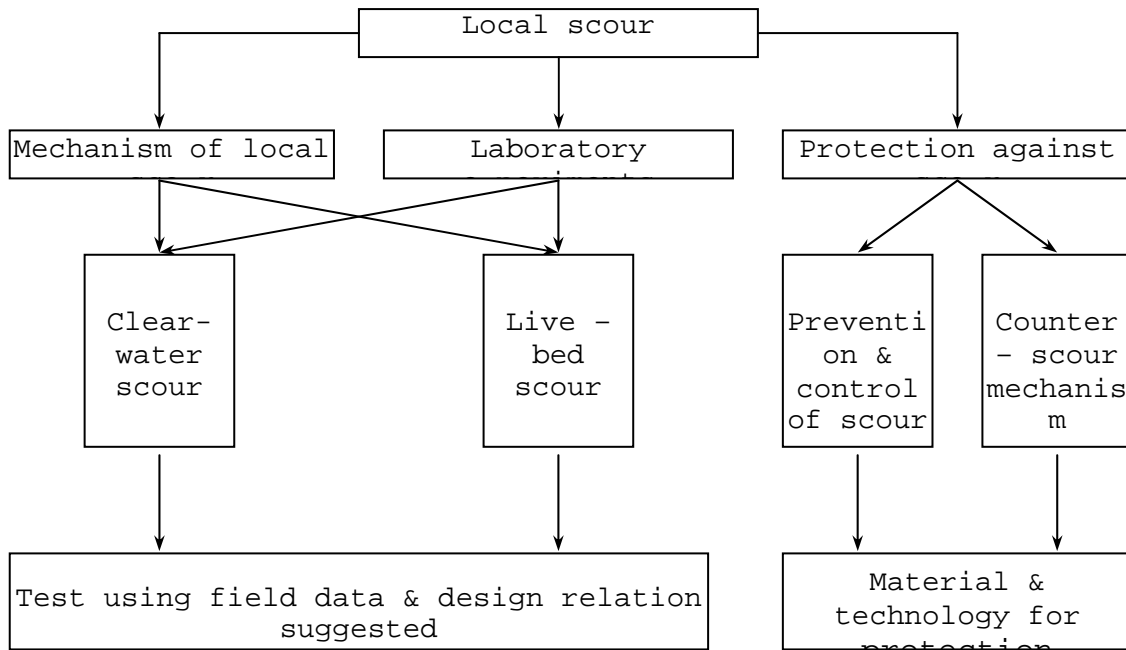


Fig.1. The flow chart for performing the research on local scour at bridge pier

3. Flow visualization by paint impression

Flow pattern near the bed & pier by paint impression method are obtained. Firstly, steady flow for each flow condition as required is set up. Then pier model alone & pier model with device model painted is tested subsequently.

3.1 Flow pattern on the plate

Original flow pattern obtained by paint impression technique has been traced & reduced in size as shown in the typical copy view in Fig.1a & Fig1.b.

For the case of pier alone, the streak-lines clearly indicate the zone of stagnation, stagnation point & zone of separation occurring on the plate due to model pier mounted on it. In the wake region, two large vortices penetrate each other as shifting downstream to form a vertex sheet behind the pier along flow direction.

For the case of pier model fitted with device model the streak lines obviously show separation point upstream of the vortex of passive device. The line of separation ahead and beneath the passive device moves down the pier & wraps the pier model. The on coming flow separates ahead of passive device, curves beneath passive device coming toward the leading part of the pier on either side of the spinal rib and pier. Separation region around pier is less compared to pier alone, representing the modification of the original horseshoe vortex.

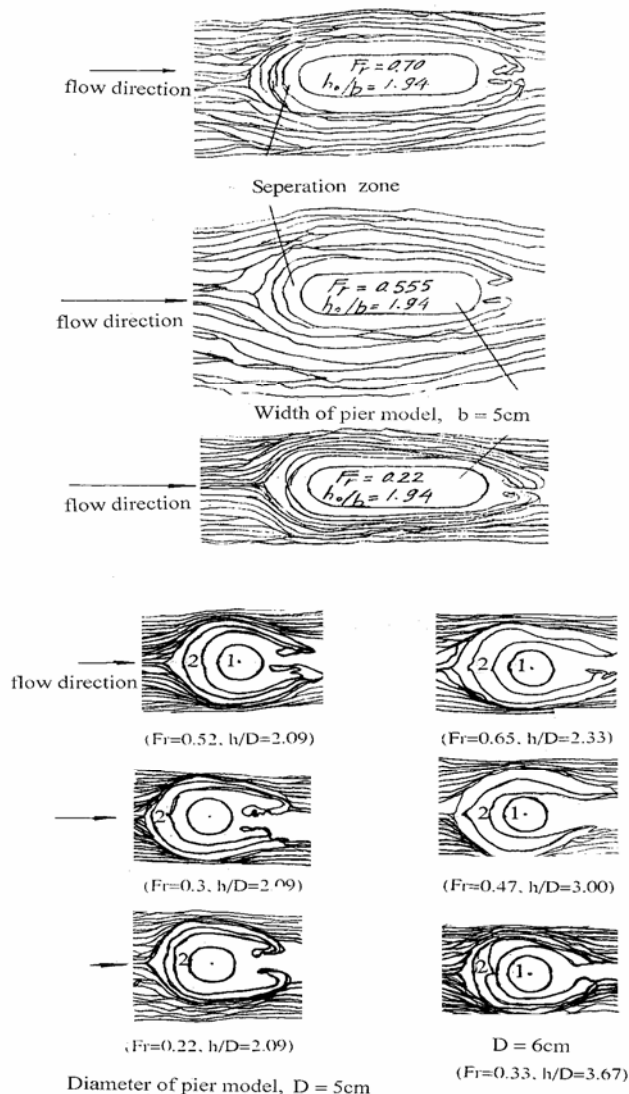


Fig.1a. Paint impression of flow pattern on the plate for pier model alone.

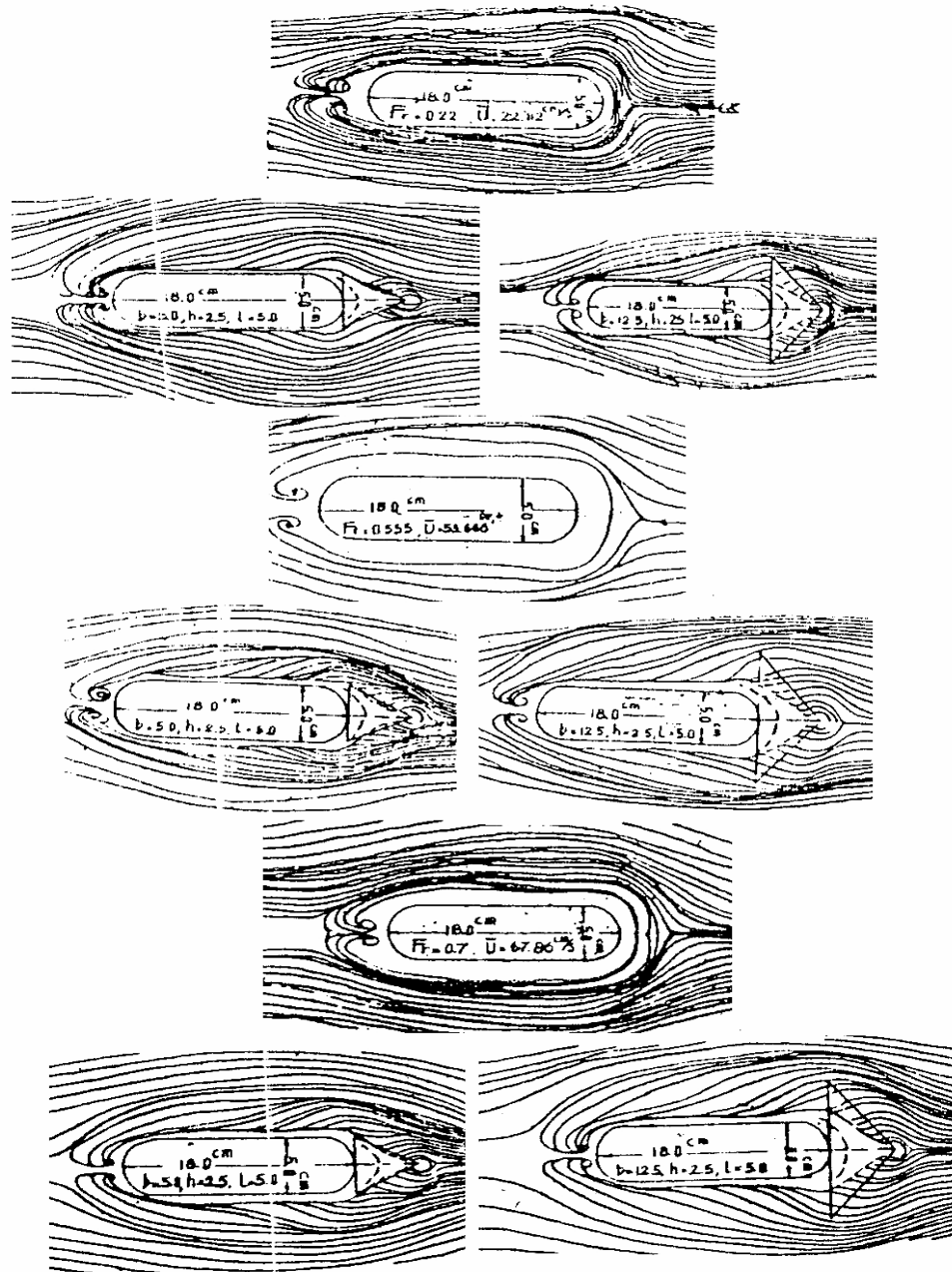


Fig.1b. *Paint impression of flow pattern on the plate for pier model alone and fitted with device model. for $Fr = 0.22; 0.55; 0.7$*

3.2 Flow pattern on the surface of the pier model

For the case of pier alone, the separation line starts just above the plate and continues up to the surface. The stagnation line starting at some distance above the plate at $\theta = 0^0$ is observed in all cases. The flow along the pier seems to be divided into two parts, upflow & downflow. Upflow is similar to flow past with free surface on the upstream flow of the pier. Downflow is affected by horseshoe vortex formed at the leading nose of the pier, near junction with the plate. Vertical separation line on the pier side surface is also observed in Fig.2.

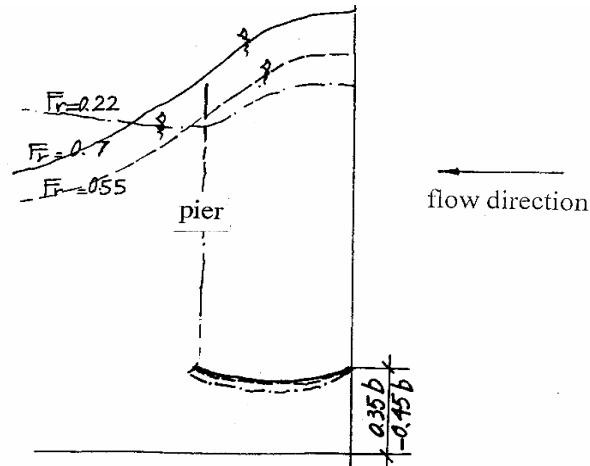


Fig.2. Vertical separation line and vortex zone on the pier side surface.

For pier model fitted with device in Fig.3. It is clear that separation point is just above device height & depends on the device model height. Depending upon the device model width flow on both sides of the pier is divided into three zones along pier height. The effectiveness of modification of original horseshoe vortex due to delta-wing-like passive device having been seen by paint impression should be illustrated by reduction scour depth in mobile bed in the next section.

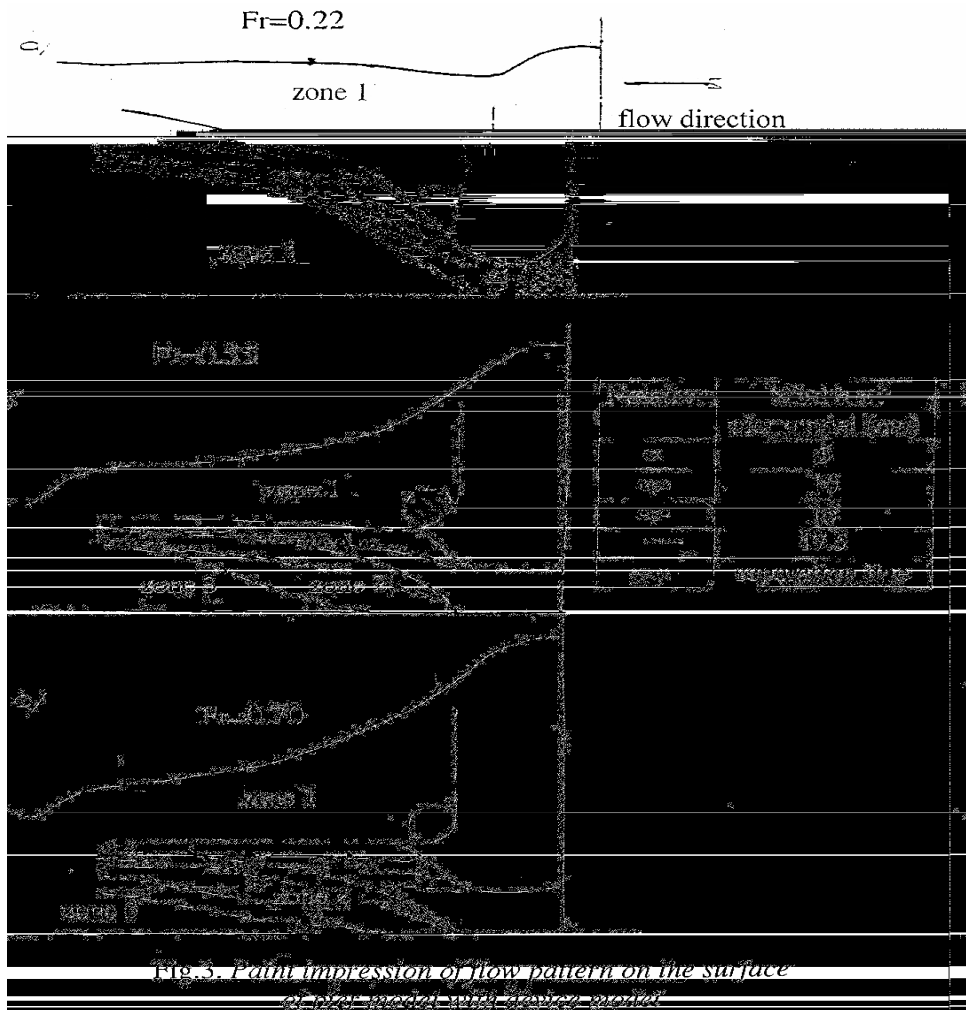


Fig.3. Paint impression of flow pattern on the surface of pier model with device.

4. Pressure distribution

The pressure on the bottom plate and on the surface of pier model were also determined with using the piezometers.

A pressure coefficient C_p is used in place of the measured pressures and defined as flows:

$$C_p = \frac{p - p_0}{\frac{1}{2} \rho u_0^2} \quad (1)$$

Where p is local pressure at any point in the model, p_0 is a reference undisturbed flow static pressure measured for upstream of the model, u_0 is the undisturbed flow maximum velocity of the approach flow, and ρ is the density of flowing fluid.

A detailed study of the pressure distribution on the plate & the surface of the pier model has been conducted. Contours of constant pressure coefficient have been drawn as shown Fig.4.

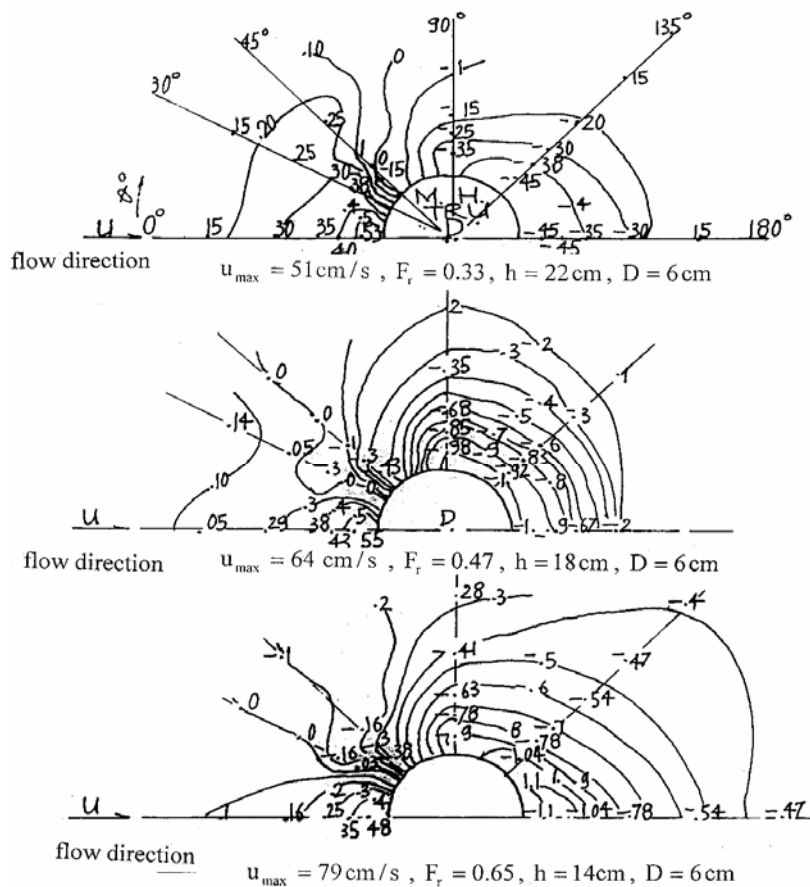


Fig.4. Pressure contours on plate before scour

From this pressure distribution it can be observed that the positive pressure occurs on the plate at $\approx \pm 35^\circ \div 45^\circ$. The negative pressure contours close on the surface forming an elliptical shape. The maximum negative pressure coefficient occurs around $\theta = 180^\circ$ while the maximum positive pressure occurs within the range $\theta = 0^\circ \div 12^\circ$.

A typical pressure contour obtained from the surface pressure distributions on the surface of the cylinder model is shown in Fig.5. It may be noted that the pressure gradually increases at $\theta = 0^\circ$ from the junction of the plate to approximately the edge of the boundary layer, similarly to the value observed from paint impression on the cylinder model surface. The pressure above the boundary layer depth remain fairly constant at $\theta = 0^\circ$. The contours of zero pressure occur around the range $\theta = 35^\circ \div 45^\circ$.

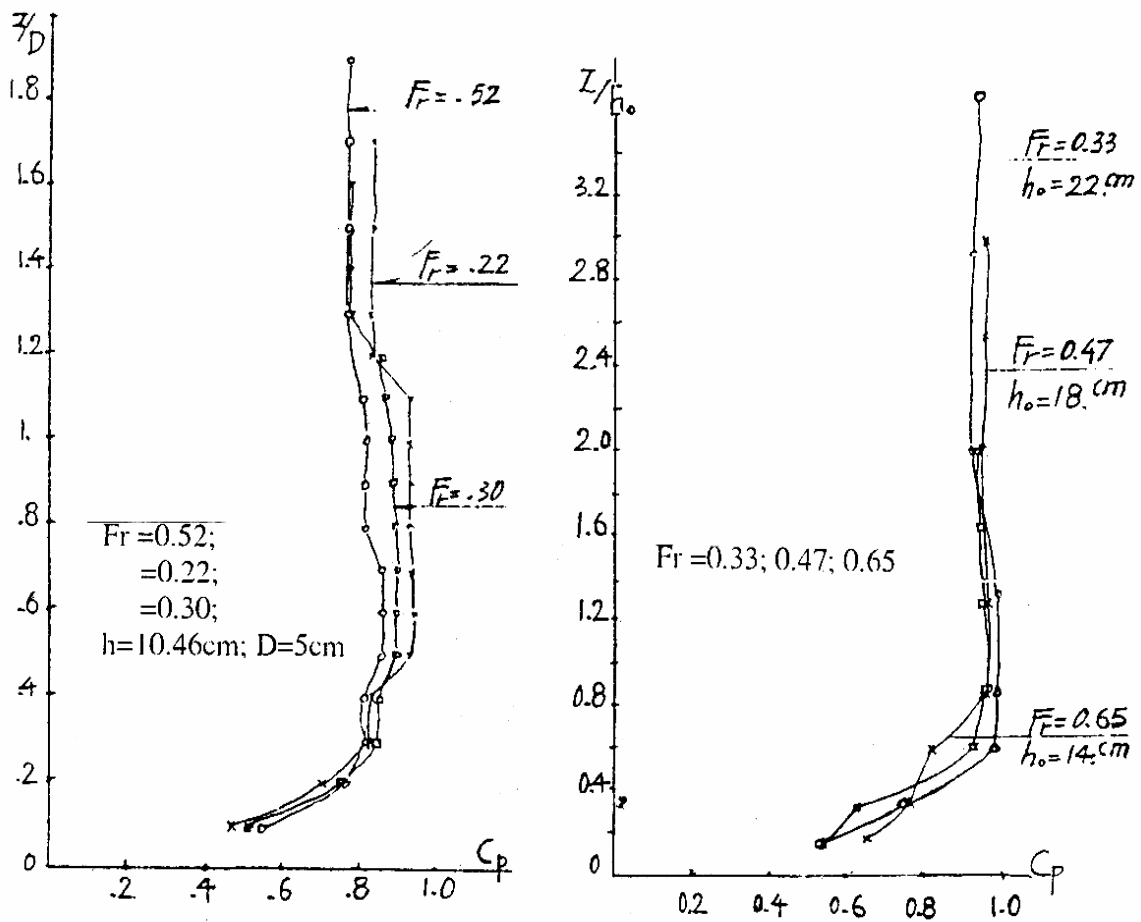
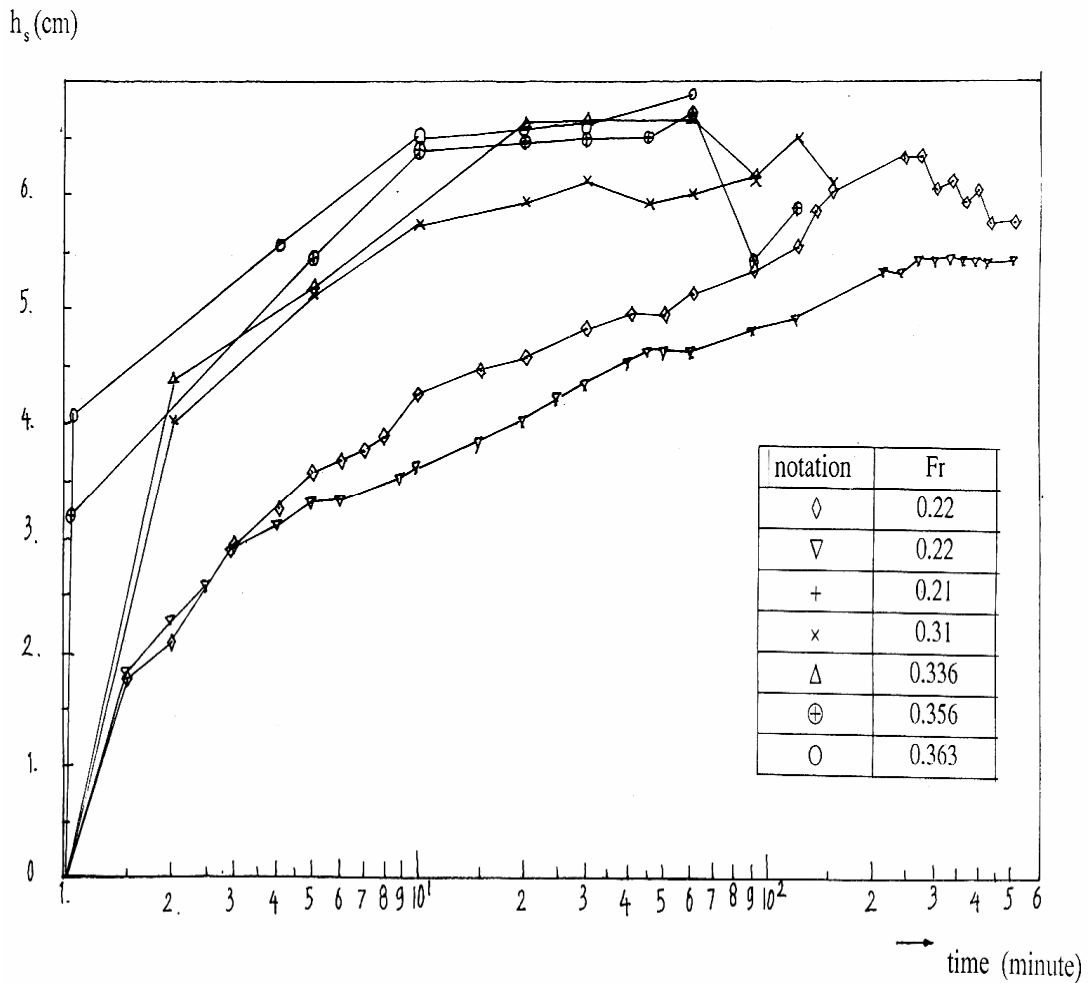


Fig. 5 . Pressure coefficient variation along the line of symmetry or $\theta = 0^\circ$ on pier model surface.

5. Maximum scour depth & scour depth as function of time

The flow field involved water & sediment movement around a cylindrical pier is too complicated, especially with the formation & the development of the scour hole. In the second phase of study, the rigid bed was removed & the bed filled up with uniform sand of 14cm thickness allowed to scour. The development of scour is recorded for pier model alone and pier filled with type of scour protection-passive device applied to the leading nose of pier model at mobile bed level. The results of scour depth around pier model for all desired purposes were shown in Fig.6a, Fig.6b, Fig.9a, Fig.9b.



*Fig.6a. Variation of scour depth versus time for pier model alone
($b=5\text{cm}$, $d_{50}=0.155\text{mm}$, $t=27^{\circ}\text{C}$)*

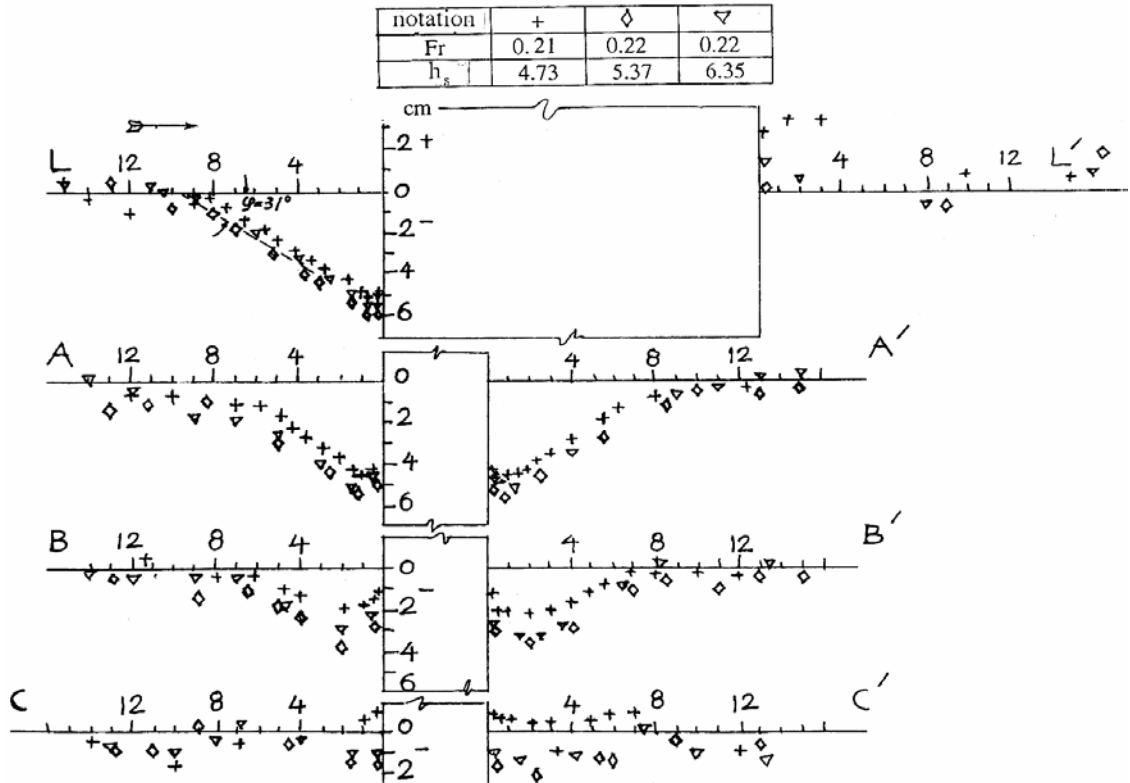


Fig.6b. Scour hole shape and depth around the round nosed pier model for width $b = 5\text{ cm}$, $Fr = 0.21 ; 0.22$.

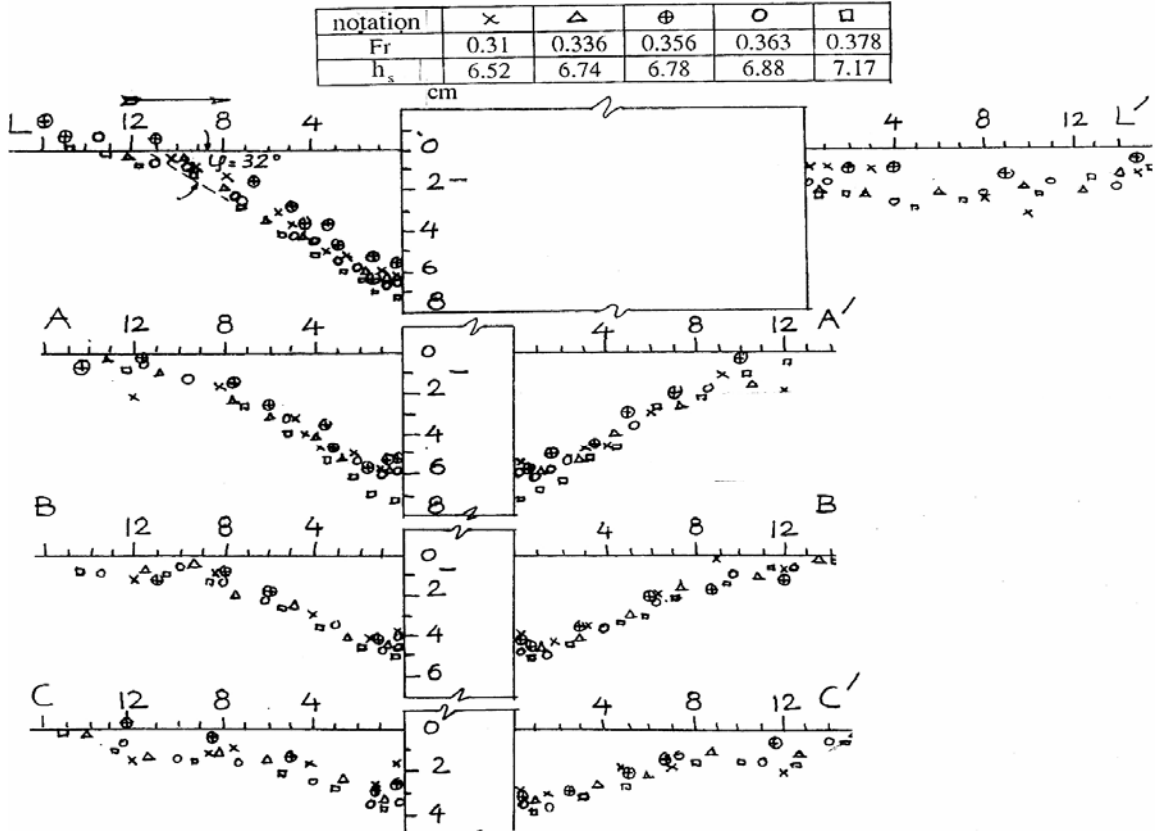


Fig.6b. Scour hole shape and depth around the round nosed pier model for width $b = 5\text{ cm}$, $Fr = 0.31; 0.336; 0.356; 0.363; 0.378$

From Fig.6a it may be observed that the data appear to plot on three curved segments on semi-logarithmic graph. The first steep segment is associated with rapid scouring by the downflow. The downflow digged sediment around the front nose of the pier model by forming different grooves.

The second slightly steep segment shows the development of the scour-hole as the horseshoe vortex moves away from the cylinder & grows in strength. The last segment describes the equilibrium local scour depth due to ripple or dunes formed on the bed by interaction between flow & sediment. In general local scour depth varies with the passing of a ripple or dune. The scour value is often less than maximum just by or ripples or dunes reach the pier.

6. The diameter of the primary forced vortex

An attempt was made to relate the diameter of the primary forced vortex to the flow depth and the pier diameter (or pier width) measured from paint impression on the flat plate. All the data collected during the study and data from investigator. Qadar and Muzzammil were given in Table 2, and have been used. The fitting of a straight line by using logarithm of the variables have been done by the method of least square. The regression line computation are made in Table 2 also and is given by:

$$\log\left(\frac{D_f}{h_0}\right) = -0.8\log\left(\frac{h_0}{b}\right) - 0.6 \quad (1a)$$

or
$$D_f = 0.25b^{0.8}h_0^{0.2} \quad (1b)$$

The correlation coefficient $r = 0.92$ which indicates a close linear relation & the straight line plot is shown in Fig.7.

Where:

b : the pier width or pier diameter.

h_0 : the flow depth

Eq.(1b) may be seen to be valid for a pier in a wide channel.

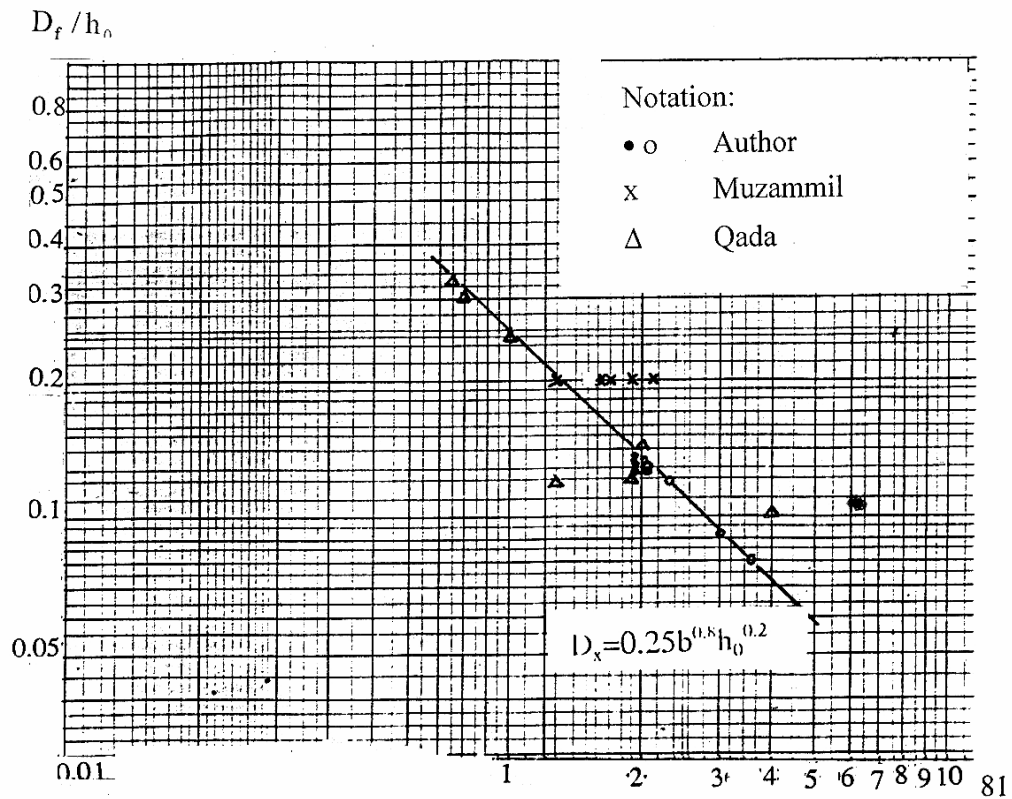


Fig.7. Variation of $(\frac{D_f}{h_0})$ with $(\frac{b}{h_0})$ in uniform flow

Table 2. Computation of diameter of forced vortex

Order	Width, b(cm)	$\frac{h_0}{b}$	$\frac{D_f}{h_0}$	$\lg(\frac{h_0}{b})$	$\lg(\frac{D_f}{h_0})$
(1)	(2)	(3)	(4)	(5)	(6)
1	5.0	1.94	0.134	0.2878	-0.873
2	5.0	1.94	0.129	0.2878	-0.889
3	5.0	1.94	0.129	0.2878	-0.889
4	6.0	3.67	0.080	0.5647	-1.097
5	6.0	3.00	0.093	0.4771	-1.032
6	6.0	2.33	0.118	0.3674	-0.928
7	5.0	2.09	0.130	0.3201	-0.886
8	5.0	2.09	0.131	0.3201	-0.883
9	5.0	2.09	0.131	0.3201	-0.883
10	2.5 – 15.0	4.00	0.100	0.6021	-1.000
11	2.5 – 15.0	1.90	0.120	0.2788	-0.921
12	2.5 – 15.0	2.00	0.140	0.3010	-0.854
13	2.5 – 15.0	1.30	0.190	0.1139	-0.721
14	2.5 – 15.0	1.00	0.250	0.0000	-0.602
15	2.5 – 15.0	0.80	0.300	-0.0969	-0.523
16	2.5 – 15.0	0.75	0.330	-0.1249	-0.481
17	5.0	2.16	0.200	0.3345	-0.699
18	5.0	1.90	0.200	0.2788	-0.699
19	5.0	1.70	0.200	0.2304	-0.699
20	5.0	1.45	0.200	0.1614	-0.699
21	5.0	1.30	0.200	0.1139	-0.699

where: 1 – 9: Author data; 10 – 16: Qadar data; 17 – 16: Muzzammil data

7. The most effective dimension of delta-wing-like passive device

The basic idea of delta-wing-like passive device introduced at a negative angle of attack at junction of the leading nose of pier model was to counter and modify the sense of rotation of the original horseshoe vortex of the pier. These vortices have sense of rotation opposite to original vortices of horseshoe shape generated without passive device. The change in sense of rotation or vortices tend to pile up to the sediment near pier surface, thus tending to alleviate the local scour almost all round the pier. This idea has been illustrated by conducting a series of experiments for choosing passive device dimensions & finding the reduction of scour depth. All experimental data have been collected. The variation of length, width and height of passive device based on effective hydraulic reason namely maximum local scour depth, extent of scour hole & location of maximum local scour depth in plan is shown in Fig.8 & Fig.9a, Fig.9b.

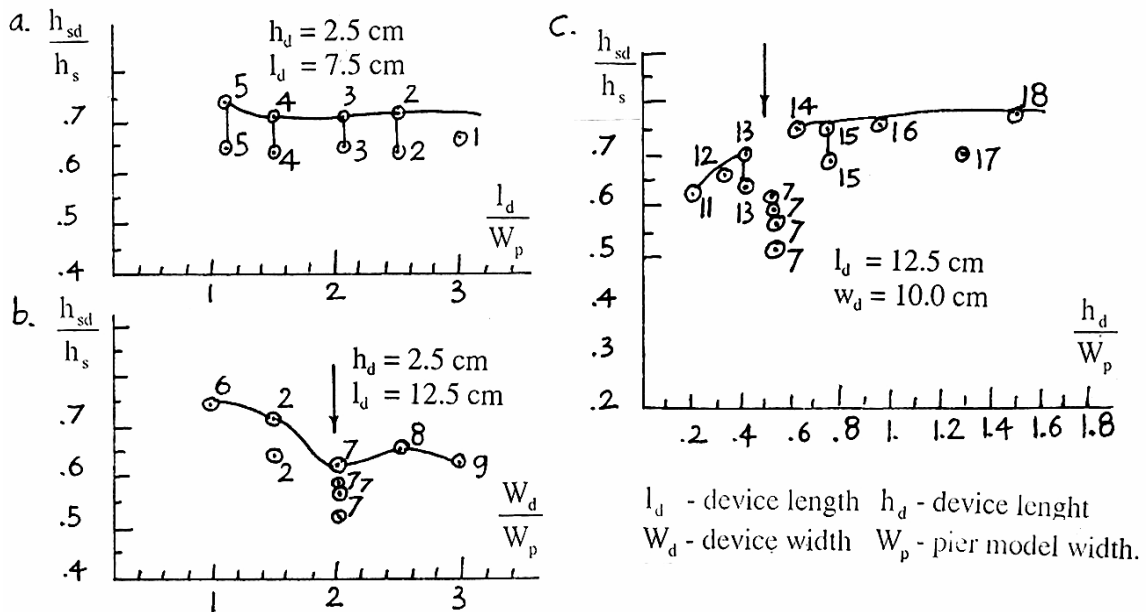


Fig.8. The most effective dimensions of delta-wing-like passive device based on effective hydraulic reason.

8. Reduction scour due to passive device

The change of sense of the scour depth around pier model and variation of the scour depth with time for pier model with passive device compared to pier model alone is shown in Fig.9a and Fig.9b. From Fig.9a it can be stated that the flow while meeting passive device nose it appears as two streamwise streaks to wrap around

the leading edge of the passive device and become stronger as they move beneath the wing or either side of the vertical spinal rib and push sediment towards the pier. Also along all other verticals within the fluid affected by passive device, there would be a vertical pressure gradient. These pressure gradients give rise to vertical secondary flows. On the upstream side along the edges of delta-wing-like passive device these secondary flow are downward at least within the layers of fluid affected by model device height. This leads to an increase of the fluid velocity of counter rotating vortex in the vicinity of device junctioned with pier. Thus, sediment is no longer far away from the pier but is pushed towards the pier. However the residual original horseshoe vortex also exists beneath the passive device near leading nose of the pier model but its strength is reduced considerably. That is why scour exists beneath the passive device, and maximum scour depth reduction is around 40 to 50 percent under these experimental flow conditions.

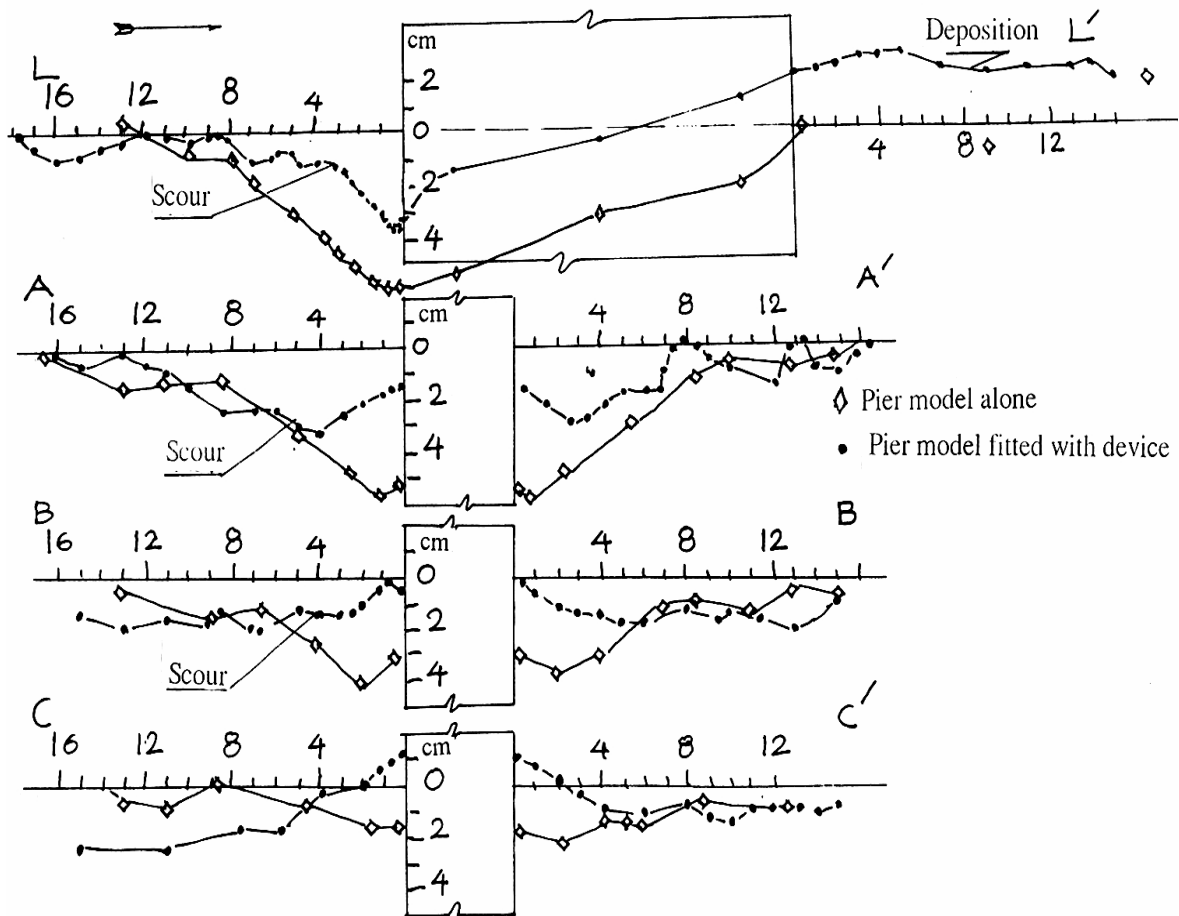


Fig.9a. The change of sense of scour depth and reduction scour depth around pier model fitted with device.

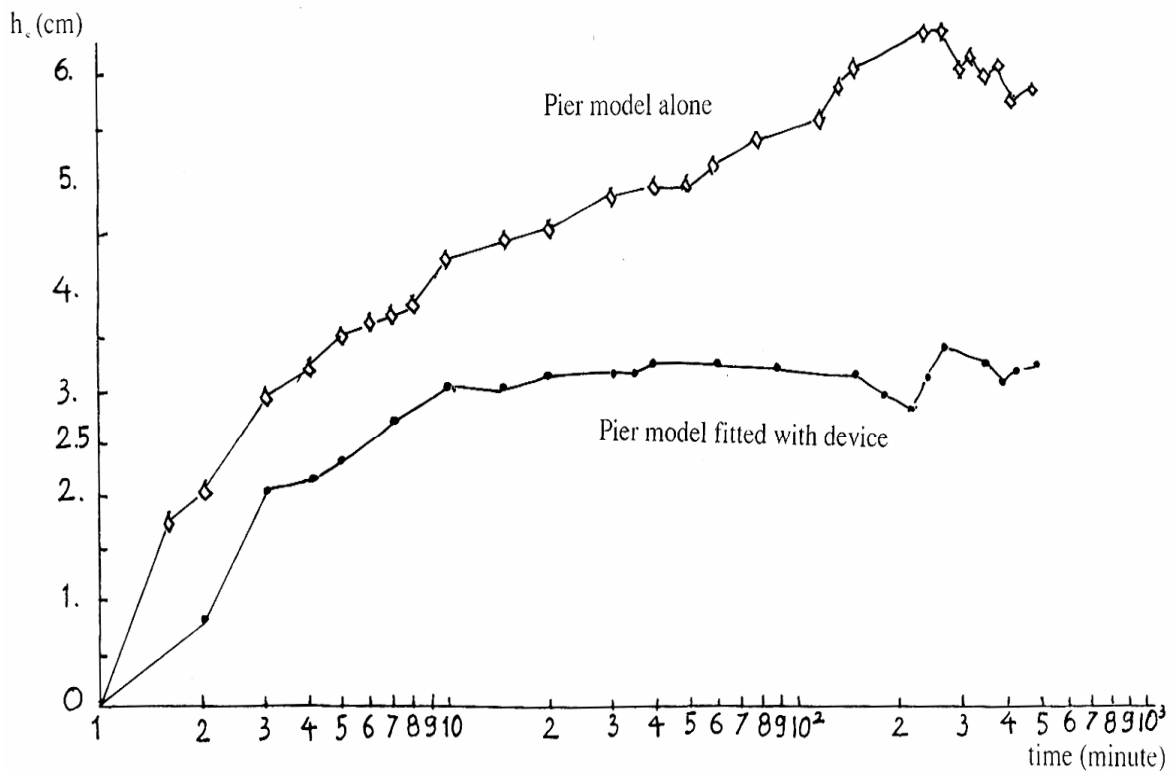


Fig.9b. Comparison of scour depth versus time for pier model alone & fitted with device

9. Scour protection using flexible mat placed around the pier model by Pr. Dr. Nguyen Xuan Truc

Pr. Dr. N.X.Truc et al (1980 ÷ 1981) has an idea of using a heavy completely flexible mat to place around the pier as the best protection device against scour.

Flexible mat mixture consist of some materials given in the Table 3

Table 3

Oder	Material	Percent
1	Iron scrap with a size of 2 ÷ 3mm	17 ÷ 79
2	Bitumen with Pn = 40 ÷ 60	15 ÷ 20
3	Lubricant oil	2 ÷ 4
4	Cement	4 ÷ 5

For all the test, the pier model diameter of 9.6cm under flow condition of 18cm water depth, 18l/s discharge and 20cm/s velocity was kept.

Deepest scour for all tests performed are summarized in Table 4.

Table 4. Summary of tests result deepest scour at pier

Type of protection \ Location	Nose	Side	Rear
No protection	8.5cm	8.0cm	7.4cm
Concrete collar	0	0	1.8cm
Flexible	0	0	0
Bag of iron scrap	0	0	0

It should be noted that in general, the results demonstrated the validity of the requirements for effective protection. It means that mat is to be used around the pier to keep material from washing away, it should be impervious, flexible, extensible and contractible in such way that it can lay on a non-planar bed of complicated shape, maintaining contact at every point. He also gave an excellent review of scour protection work of D.M.Zgorsky (Kiev Bridge & Road University), N.A.Mikhailov (Moskva).

10. Mathematical model

The dominant feature of the flow near pier is the large-scale eddy structure, or the system of vortices, which develops about the pier. These vortex systems are the basic mechanism of local scour. In this report, circulation of the primary forced vortex is based on the kinetic energy difference between boundary layers on both sides of the pier and undisturbed approach flow coming to the pier in steady flow. To get the forced vortex circulation, the following simplified assumptions were made regarding the mean description of geometric & hydraulic characteristics of the primary forced vortex.

- (1). The primary forced vortex at the pier nose is circular shape.
- (2). As the scour hole develops, the primary vortex sinks into it and expands, then the shear stress beneath the vortex system decreases, until at the equilibrium scour depth the shear stress is not large enough to move any sediment out of the scour hole.

(3). The vortex circulation remains approximately constant during the scouring process, since more of the cylinder surface becomes exposed. This effect will tend to decrease the angular velocity ω . Thus, since r increases and ω decreases, it seems reasonable to assume that vortex radius increases as the scour depth increases and circulation Γ remains approximately constant in scour process.

These assumptions permit to write:

$$\Gamma_f = \Gamma \quad (2)$$

where Γ_f and Γ is the primary forced vortex circulation and the scour hole vortex circulation, respectively.

10.1 Determination of the primary forced vortex circulation Γ_f

While a cylindrical pier set in the uniform flow, the hydrodynamic force exerted by the fluid on it is:

$$F_D = C_D \rho_f \frac{V^2}{2} Dh \quad (3)$$

in which V is the approach mean velocity; D is pier diameter; h is flow depth; ρ_f is mass density of the fluid; Dh is the projected area of the pier and C_D is the drag coefficient of the pier at the pier Reynolds number corresponding to V . The power supply per second due to this force is:

$$P = F_D V \quad (4)$$

Substituting (3) in to (4) gives:

$$P = C_D \rho_f \frac{V^2}{2} Dh V \quad (5)$$

Relation (5) means kinetic energy exerted on the pier.

As assuming that forced vortex in the circular shape with ω as the angular velocity and may be represented by a circular motion, then the kinetic energy of the forced vortex is:

$$E_f = \frac{I_f \omega^2}{2} \quad (6)$$

where I_f is the second moment (or inertial moment) of the forced vortex about an axis through its centroid:

$$I_f = \frac{m_f r_f^2}{2} \quad (7)$$

$$m_f = 2(kV)\rho_f \pi r_f^2 \quad (8)$$

in which m_f is the forced vortex discharge.

Referring to (7) and (8), (6) is rewritten as:

$$E_f = \frac{1}{2}(kV)\rho_f \pi r_f^4 \omega^4 \quad (9)$$

where k is factor depending upon redistribution & increment of velocity in boundary layers on both sides of the pier.

The change of the kinetic energy crossing a control surface in boundary layers of the pier and the approaching kinetic energy to the pier should be equal to the forced vortex kinetic energy:

$$\Delta E = E_b - E_a = \frac{k^2 V^2}{2} \rho_f DhV - \frac{V^2}{2} \rho_f DhV \quad (10)$$

$$\text{or } \Delta E = \frac{1}{2} V^2 (k^2 - 1) \rho_f DhV = \frac{k^2 - 1}{C_D} P \quad (11)$$

in which E_b and E_a is the boundary layer kinetic energy and approaching kinetic energy to the pier, respectively.

Equating (9) and (11), and noting that $\omega r_f = V_{\theta f}$ and $\Gamma_f = 2\pi r_f V_{\theta f}$ yields the primary forced vortex circulation:

$$\Gamma_f = \frac{3.545}{\sqrt{C_D}} \sqrt{\frac{k^2 - 1}{k}} V \sqrt{Dh} \quad (12)$$

10.2 Vortex circulation in the scour hole

The primary forced vortex systems produce high shear stress on the sediment river bed beneath them and a scour hole form beneath such systems. Throughout the process of scour, the upstream part of the scour hole develops rapidly and can be approximated as the shape of a frustrum of an inverted cone with slope equal to the

angle of repose of the bed material under erosion conditions. Two types of scour can be indentified.

(1). Clear-water scour, for it movement of sediment only takes place in the vicinity of the pier and an equilibrium is reached when the combined effect of the temproral mean shear stress, the weight component and the turbulent agitation are equilibrium everywhere or velocity fall below the value needed for movement of sediment. Particles on the surface of scour hole may be occasionally moved but are not carried away.

(2). Live-bed scour or scour with continuous sediment motion, where the hole river bed is in motion. In this case, an excess shear stress or velocity must exist to transport the sediment through the scour hole; the equilibrium scour depth is reached when the inflow of sediment into the scour hole is equal to the outflow of sediment from the scour hole.

Assuming that in both scour cases, the vortex system within the scour hole may be represented by a circular forced vortex motion of radius r and maximum circulation Γ . Then:

$$\Gamma = 2\pi r^2 \omega_c \quad (13a)$$

or

$$\Gamma = 2\pi r^2 V_c \quad (13b)$$

where V_c is the tangential velocity at the edge of the vortex. Assume that the radius of this vortex is half of maximum scour depth at equilibrium scour depth $r = \frac{h_c}{2}$,

$A = \pi r^2$ is the cross-section area of the vortex in the scour hole. V_c is the tangential vortex velocity at the equilibrium scour depth and its use here as the “characteristic” velocity with meaning sediment averaged-disturbed velocity in the scour hole:

$$V_c = \sqrt[3]{gh\omega_d} \left(\frac{h}{d}\right)^{0.06} \quad (14)$$

Under these latter conditions, the maximum circulation (13) will be in a new form:

$$\Gamma = 4A_s \frac{V_c}{h_s} \quad (15)$$

10.3 Scour depth theoretical relation

Equating Γ_f in (12) and Γ in (15) for condition of equilibrium scour depth, one gets:

$$\frac{A_s}{h_s} = \frac{0.886}{\sqrt{C_D}} K_1 \sqrt{Dh} \frac{V}{V_c} \quad (16)$$

or simplified to:

$$h_s = 1.13 \frac{1}{\sqrt{C_D}} K_1 \sqrt{Dh} \frac{V}{V_c} \quad (17)$$

where $K_1 = \sqrt{\frac{k^2 - 1}{k}}$

relation (17) in the dimensionless form:

$$\frac{h_s}{D} = 1.13 \frac{1}{\sqrt{C_D}} K_1 \sqrt{\frac{h}{D}} \frac{V}{V_c} \quad (18)$$

This means that the scour depth h_s will depend mainly on the ratio of mean velocity to mean “characteristic” velocity in the scour hole, flow depth, pier diameter, and the relative grain size through V_c .

11. Identification of factors in relations (16) – (18)

(1). Pier drag coefficient C_D

All bridge pier models conducted in two phases of investigation were at pier Reynolds number ranging in value from 12.79×10^3 to 50.32×10^3 for flat plate and from 12.26×10^3 to 21.64×10^3 for mobile bed. The value of these Reynolds number is larger than 10^3 and less than 10^5 , then the value C_D is 1.0

(2). Factor $K_1 = \left(\frac{k^2 - 1}{k} \right)^{0.5}$

The results of this study show $k = 1.35 - 1.45$, while other investigators such as Juravlev gave $k = 1.7 - 2.0$, Arkhipov gave $k = 1.3 - 1.7$, N.X.Truc gave $k \leq 1.5$. These values of k leading to K values ranging from 0.73 to 1.2.

(3). Analysis of experimental data varified $C_D = 1$, angle of frustum of scour hole to be equal to the angle of repose of bed sediment size ranging from 0.155mm to

0.58mm, $\phi \approx 33^\circ$. This angle makes the cross-sectional area of this vortex presented by the circular forced vortex motion to be equal to the area of cross section of the scour hole, then $\frac{1.13K_1}{\sqrt{C_D}} = K$ and relation (18) becomes:

$$\frac{h_s}{D} = K \sqrt{\frac{h}{D}} \frac{V}{V_c} \quad (19)$$

(4). 103 field data and experimental data including data from Ettema, Shen et al, Charbert & Engeldinger, Knight for clear-water verified that $K = 1.24$ and exponent of $\frac{V}{V_c}$ is 0.77.

(5). 85 field data verified that $K = 1.11$ and exponent of $\frac{V}{V_c}$ being equal to 1.0 for live-bed scour.

12. Suggestion for practical design

From the material presented it is concluded that the scour depth may be described by a function of the form for practical design:

$$h_s = K \sqrt{Dh} \left(\frac{V}{V_c} \right)^n K_\alpha K_{sh}, \quad (m) \quad (20)$$

where:

$K = 1.24$, $n = 0.77$ for $V < V_c$

$K = 1.11$, $n = 1.0$ for $V \geq V_c$

K_α, K_{sh} = correction factors for angle of attack, pier shape

V = mean velocity of flow directly upstream of pier (m/s)

$$V_c = \sqrt[3]{gh\omega_d} \left(\frac{h}{d} \right)^{0.06} \quad (m/s)$$

This equation will predict the maximum scour depth of local scour around a pier. The lateral dimensions of the scour hole are primarily dependent of the scour depth & bed material.

This equation is not included a case of armoring bed around pier and nonuniform sediments as well.

13. Pr. Dr. N.X.Truc et al (1980 - 1981)

N.X.Truc et al used theorem of Vaschy-Buckingham and method of regression analysis to write a relation based on available field data from Viet Nam, USSR and some other countries.

$$h_s = 0.97K_d b^{0.83} h^{0.17} \left(\frac{V}{V_0} \right)^{1.04} \quad (\text{m}) \quad (21)$$

for clear-water scour ($V < V_0$)

$$h_s = 0.52K_d b^{0.88} h^{0.12} \left(\frac{V}{V_0} \right)^{1.16} \quad (\text{m}) \quad (22)$$

for live-water scour ($V \geq V_0$)

where:

K_d = correction factor for pier shape, $K_d = 0.1K_\zeta$

K_ζ = correction factor for pier shape based on experimental data from Iaroslavtsev (USSR).

$$V_0 = 3.6(h.d)^{0.25} \quad (\text{m/s})$$

14. Tong Anh Tuan & T.D.Nghien (May, 2005)

T.A.Tuan & T.D.Nghien used the diameter of the primary forced vortex proposed in relation (1b) & available experimental & field data to develop new practical design relation:

$$h_s = Kh^{0.2} b^{0.8} \left(\frac{V}{V_c} \right)^n K_d K_\alpha K_{sh}, \quad (\text{m}) \quad (23)$$

where:

$$K_d = \text{relative sediment factor, } K_d = 1 + \frac{1}{2.7} \left(\frac{d}{h} \right)^{1/6}$$

$$V_c = \sqrt[3]{gh\omega_d} \left(\frac{h}{d} \right)^{0.06} \quad (\text{m/s})$$

b = pier width or pier diameter, (m)

V , K_α , K_{sh} as mentioned above.

$K = 1.21$, $n = 0.57$ for $V < V_c$

$K = 0.93, n = 1.5$ for $V \geq V_c$

15. Comparison with some practical design relations

21 experimental & field data for clear-water scour and 21 filed data for live-bed scour were used to make comparison of relations (20), (21), (22), (23) together with relations proposed such as relation from Juravlev (Russia), Froehlich (USA).

Results of comparison have been shown in Fig.10 & Fig.11.

Range of parameters used is given in the Table 5.

Table 5

Clear-water scour						Live-water scour					
h (m)	b or D (m)	h_{obs} (m)	V (m/s)	$\frac{h}{b}$	$\frac{V}{V_c}$	h (m)	b or D (m)	h_{obs} (m)	V (m/s)	$\frac{h}{b}$	$\frac{V}{V_c}$
0.4	0.1	0.06	0.18	0.5	0.25	1.0	1.9	2.5	1.0	0.3	1.0
to	to	to	to	to	to	to	to	to	to	to	to
15	12	5.4	2.6	7.0	1.0	8.0	3.0	6.0	3.2	2.6	1.8

where h_{obs} = depth of observation.

The comparison between the observed scour depths and the scour depth predicted by six formulas shown in Fig.10 & Fig 11 together with the values of the linear correlation coefficient, r , between the observed & predicted scour depth are also included in these figures indicates how well the proposed equations fit the data. The relative deviation, standard deviation for six equations is given in Table 6 for clear-water scour & in Table 7 for live-bed scour.

Table 6. Bias for six scour equations

Oder	Equation	Δ_{max} (%)	Δ_{min} (%)	δ (%)	Author
1	(20)	39.65	-6.55	24.14	T.D.Nghien
2	(21)	46.36	-16.24	23.91	Viet Nam Specification 220 -95
3	(23)	9.46	-32.97	15.52	T.A.Tuan & T.D.Nghien
4	(26)	49.72	-6.41	25.45	Froehlich (USA) (HEC – 18)
5	(24)	33.15	-39.08	19.83	Specification (USSR)
6	(27)	21.15	-18.41	11.72	Juravlev M.M

Table 7. Bias for six scour equation under live bed condition

Oder	Equation	Δ_{\max} (%)	Δ_{\min} (%)	δ (%)	Author
1	(20)	38.52	-27.2	19.8	T.D.Nghien
2	(22)	106.31	0.82	60.12	Viet Nam Specification 220 -95
3	(23)	29.63	-35.27	20.57	T.A.Tuan & T.D.Nghien
4	(26)	72.82	-36.42	28.85	Froehlich (USA) (HEC – 18)
5	(25)	156.05	-15.53	66.33	Specification (USSR)
6	(28)	37.27	-27.85	19.40	Juravlev M.M

From the values in Table 6 & 7 it can be noted that the bias $\Delta_{\max} = 49.72$ & $\Delta_{\min} = -39.08$ for clear-water scour; $\Delta_{\max} = 156.05$ & $\Delta_{\min} = -36.42$ for live bed scour. These biases point out the need for additional research on the scour process for both cases of scour how proposed equations to be satisfactory flow & pier conditions concerned by engineers.

Formula in specification of USSR:

$$\text{for clear-water scour: } h_s = \frac{6.2xh}{\left(\frac{V_0}{\omega_d}\right)^x} \left(\frac{V - V_i}{V_0 - V_i}\right)^{0.75} K_\alpha K_{sh}, \quad (m) \quad (24)$$

$$\text{for live bed scour: } h_s = (h + 0.014b \frac{V - V_0}{\omega}) K_\alpha K_{sh}, \quad (m) \quad (25)$$

where:

V_i = inceptive velocity (m/s)

$$V_i = V_0 \left(\frac{d}{h}\right)^y; \quad y = f\left(\frac{h}{d}\right)$$

$$x = 0.18 \left(\frac{b}{h}\right)^{0.867}$$

K_α, K_{sh} is mentioned above

d = medium sediment size

b = pier width (m)

$$\text{Froehlich: } h_s = 2.0K_1K_2K_3K_4h^{0.35}b^{0.65}Fr^{0.43} \quad (26)$$

K_1, K_2, K_3 & K_4 = correction factors for pier shape, angel of attack, bed condition and armoring, respectively.

$$Fr = \frac{V}{\sqrt{gh}}$$

Juravlev:

$$\text{for clear-water scour: } h_s = 1.1h^{0.4}b^{0.6}\left(\frac{V}{V_c}\right)^{0.67} K_\alpha K_{sh}, \quad (m) \quad (27)$$

$$\text{for live bed scour: } h_s = 1.1h^{0.5}b^{0.5}\left(\frac{V}{V_c}\right)^{1.0} K_\alpha K_{sh}, \quad (m) \quad (28)$$

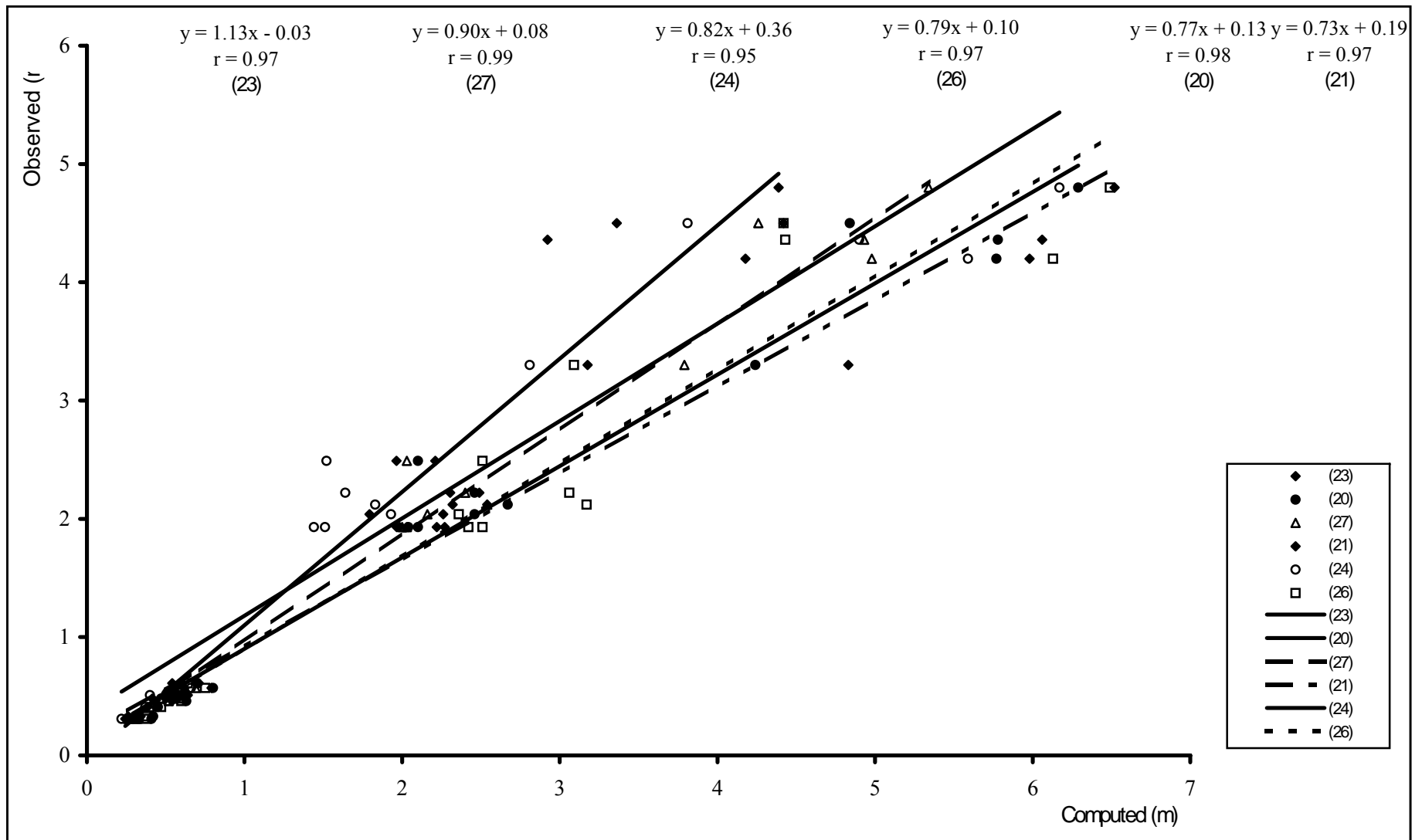


Fig.10. Comparison between Eq. (20), (21), (23), (24), (26) & (27) for clear-water scour

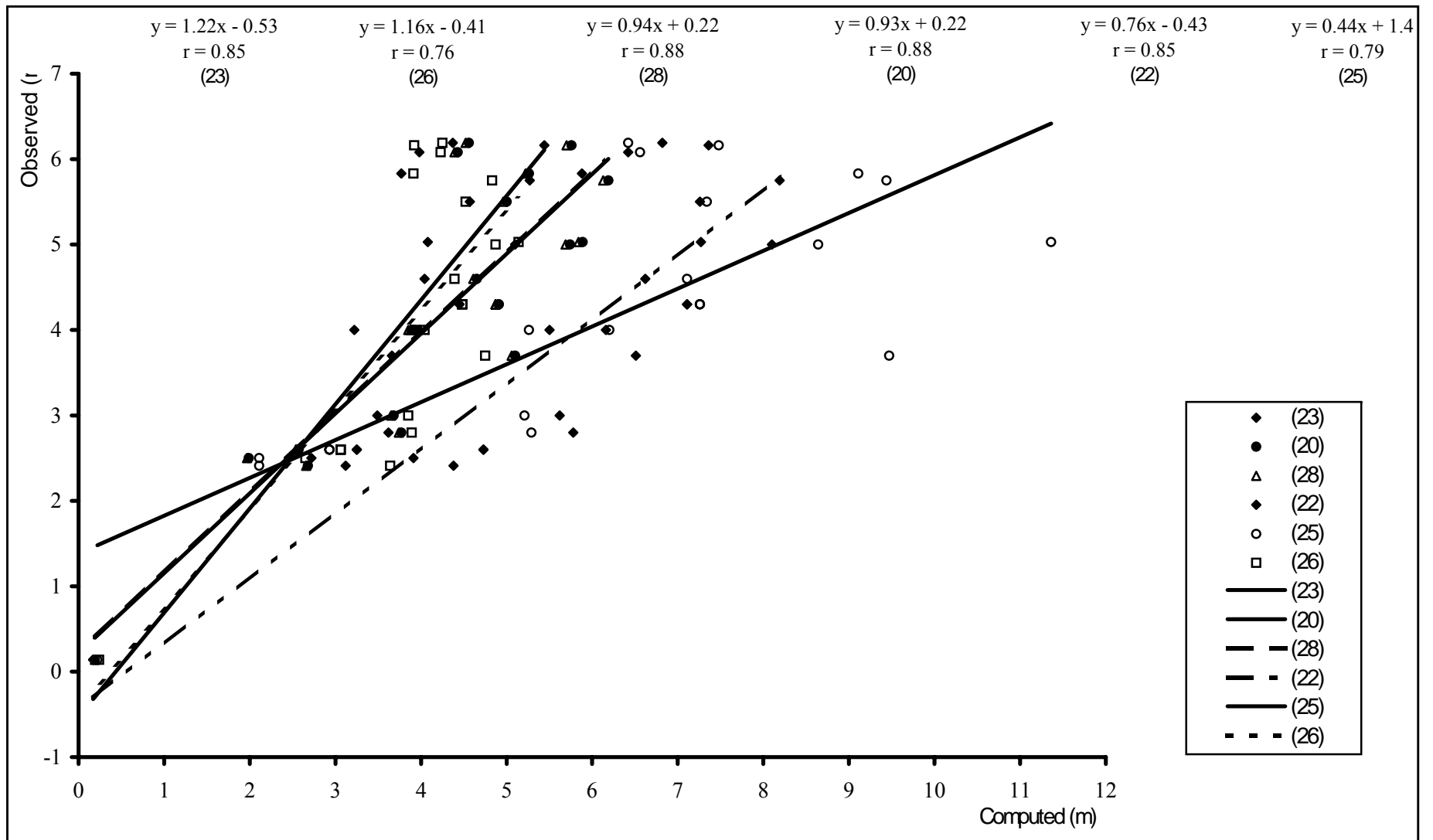


Fig.11. Comparison between Eq. (20), (22), (23), (25), (26) & (28) for live bed scour

16. Conclusion

1. The primary forced vortex in front of the pier has been considered the prime agent causing local scour at bridge pier.
2. Based on experimental data under steady flow condition the diameter of forced vortex to the flow depth & the pier diameter (or pier width) has been proposed.
3. Eq (20) has been developed for predicting maximum local scour depth in case of uniform sediment by using the change of kinetic energy crossing the control surface in boundary layers of the pier and the approaching kinetic energy to the pier for finding the primary forced vortex circulation to be equal to vortex circulation in the scour hole and available experimental & field data.
4. Eq (21) & (22) has been suggested based on available field data.
5. Eq (23) has been proposed based on forced vortex diameter in relation (1b) & available experimental & field data.
6. Delta-wing-like passive device introduced at a negative of attack at junction of the leading nose of pier for reduction of local scour depth around 40 to 50 percent under experimental condition has been proposed.
7. Plexible mat with it's material components to place around the pier as the best protection device against scour under experimental flow condition has been proposed.

References

1. T.D.Nghien (January, 1988). "Laboratory investigation of scour reduction near bridge pier by delta-wing-like passive device". M.Tech.Thesis, I.I.T Kampus, India.
2. T.D.Nghien (1992 - 1993). "Theory of local scour at bridge pier", Report, University of Transportation.
3. T.D.Nghien (2000). "Local scour at bridge pier". Ph.D.Thesis, University of Transportation.
4. N.X.Truc & N.H.Khai. "Local scour at bridge pier & design relation proposed". Transportation Journal, No 4, 1982, pp 49 - 52.
5. T.T.Xuan "Total stream flow in Viet Nam". Scie-Tech-Hydro-Meteoro. J. Hydro-Meteoro-Service of Viet Nam. No 11 (503), 2002.
6. H.N.C Breusers, G.Nicollet, H.W.Shen. "Local scour around cylindrical piers". J.of Hydr. Research (1977). No.3.